Journal of Marine Research, 42, 103–121, 1984

Wind and thermal conditions along the equatorial Pacific

by Jean-René Donguy,[1] Alain Dessier,[1] Gérard Eldin,[1]
Alain Morliere[1] and Gary Meyers[2]

ABSTRACT

Variability in heat storage of the equatorial Pacific Ocean during El Nino Southern Oscillation episodes is analyzed from subsurface temperature observations in order to show how the patterns of heat content are related to changes in the Walker Circulation. Large-scale zonal gradients in depth of the thermocline (and dynamic height) are largely in equilibrium with local zonal wind stress. Depth of the thermocline is positively correlated with mixed layer heat content and sea-surface temperature in the central Pacific during a minor El Nino/Southern Oscillation episode in 1969, indicating that the oceanic dynamic response to wind forcing as well as thermodynamic response to surface heat fluxes influence local heat storage. The distribution of heat in the mixed layer along the equator has distinctive patterns associated with pre-El Nino and mature El Nino stages. Heat is accumulated in the western Pacific during the first stage and in the central Pacific during the second. The shift in pattern is associated with a change in direction of zonal wind stress in the western Pacific. Rainfall observations show that the ascending branch of the Walker cell is always located over the region where heat is accumulated in the ocean. These observations are incorporated into a hypothetical model of the mechanism by which the equatorial ocean and atmosphere become locked into an anomalous pattern during El Nino periods.

1. Introduction

Several processes are important in controlling interannual hydroclimatic conditions along the equator. On the one hand, the zonal pressure gradient is related to the zonal wind stress. The two may be in equilibrium for sufficiently slow wind variations (Lemasson and Piton, 1968; Katz *et al.,* 1977; Halpern, 1980), or the variable wind may force transients in baroclinic structure (Meyers, 1979). In either case variability is controlled by adiabatic processes largely associated with change in depth of the thermocline. On the other hand, heat content in the equatorial area may be related to heat fluxes through the sea surface (Weare *et al.,* 1981; Weare, 1983), as well as wind-forced upwelling. Descriptive studies of the heat content have demonstrated the existence of large, coherent signals (Merle, 1980a,b; Hénin and Donguy, 1980), largely related to change in depth of thermocline. These studies did not attempt to

1. Groupe SURTROPAC, Centre ORSTOM de Nouméa, B.P. A5 Nouméa, New Caledonia.
2. Scripps Institution of Oceanography, University of California at San Diego, LaJolla, California, 92037, U.S.A.

Table 1.

Cruise	Date		Longitude	γ	T_x
*Equapac***	Aug–Oct	1956	140°E–170°E	$+2{,}3\ 10^{-7}\ ms^{-2}$	$-4{,}2\ 10^{-2}\ Nm^{-2}$
*Equapac***	Aug–Sept	1956	135°W–175°W	$+5{,}0\ 10^{-7}\ ms^{-2}$	$-10{,}0\ 10^{-2}\ Nm^{-2}$
*Igy***	Jan–Feb	1958	147°E–157°E	$-3{,}6\ 10^{-7}\ ms^{-2}$	$-4{,}1\ 10^{-2}\ Nm^{-2}$
Composite[1]					
Cruise**	Sept–Dec	1961	140°W–176°W	$+7{,}4\ 10^{-7}\ ms^{-2}$	$-5{,}4\ 10^{-2}\ Nm^{-2}$
*Alize**	Nov–Dec	1964	100°W–140°W	$+6{,}0\ 10^{-7}\ ms^{-2}$	$-3{,}4\ 10^{-2}\ Nm^{-2}$
*Alize**	Feb–March	1965	145°W–161°E	$+4{,}7\ 10^{-7}\ ms^{-2}$	$-6{,}0\ 10^{-2}\ Nm^{-2}$
*Caride 1**	Sept–Oct	1968	135°W–156°W	$+8{,}4\ 10^{-7}\ ms^{-2}$	$-8{,}1\ 10^{-2}\ Nm^{-2}$
*Caride 2**	Nov–Dec	1968	137°W–157°W	$+8{,}1\ 10^{-7}\ ms^{-2}$	$-8{,}2\ 10^{-2}\ Nm^{-2}$
*Caride 4**	June–July	1969	137°W–155°W	$+5{,}2\ 10^{-7}\ ms^{-2}$	$-5{,}6\ 10^{-2}\ Nm^{-2}$
*Caride 6**	Nov–Dec	1969	151°W–168°W	$+3{,}1\ 10^{-7}\ ms^{-2}$	$-4{,}1\ 10^{-2}\ Nm^{-2}$
*Cassiopee**	Jan–Feb	1970	140°W–156°W	$+4{,}0\ 10^{-7}\ ms^{-2}$	$-9{,}8\ 10^{-2}\ Nm^{-2}$
*Foc 1**	Jan–Feb	1971	143°E–154°E	$+5{,}1\ 10^{-7}\ ms^{-2}$	$-1{,}1\ 10^{-2}\ Nm^{-2}$
*Foc 2**	June–July	1971	143°E–154°E	$+2{,}5\ 10^{-7}\ ms^{-2}$	$-2{,}9\ 10^{-2}\ Nm^{-2}$
*Aliopee***	Aug–Sept	1975	150°W–165°E	$+6{,}4\ 10^{-7}\ ms^{-2}$	$-12{,}4\ 10^{-2}\ Nm^{-2}$
*Eponite 2***	Aug–Sept	1976	163°E–174°E	$+2{,}0\ 10^{-7}\ ms^{-2}$	$+0{,}2\ 10^{-2}\ Nm^{-2}$

*Individual stations on the equator.
**Averages 2N–2S
(1) WODC 090039
900065
310884
310214

separate the adiabatic and diabatic effects, although the importance of this distinction has been recognized (Emery, 1976; Stevenson and Niiler, 1983). The distinction is established in this article with regard to the El Nino-Southern Oscillation phenomenon, which is now recognized as the dominant signal in historical hydrographic time series for the tropical Pacific (Masuzawa and Nagasaka, 1975; White and Hasunuma, 1980; Donguy *et al.*, 1982).

2. Wind stress and zonal pressure gradient

The Centre ORSTOM de Noumea has carried out several cruises along the equator in the central and western Pacific since 1964. Cruise names and dates are given in Table 1. Equatorial sections of temperature, salinity, and nutrients for all the cruises have been published (Anonymous, 1980, 1981), but only the *Alize* cruise has been described in detail (Lemasson and Piton, 1968). Several of the temperature sections are shown in Figure 1. In addition to these synoptic sections, quasi-synoptic, composite equatorial sections can be formed from other nearly synchronous cruises (*Equapac,* 1956; *Igy,* 1958; 1961). The observations from all the available cruises are used in this section to describe how wind stress, zonal pressure gradient, and depth of the thermocline are related during variability with very long time scales.

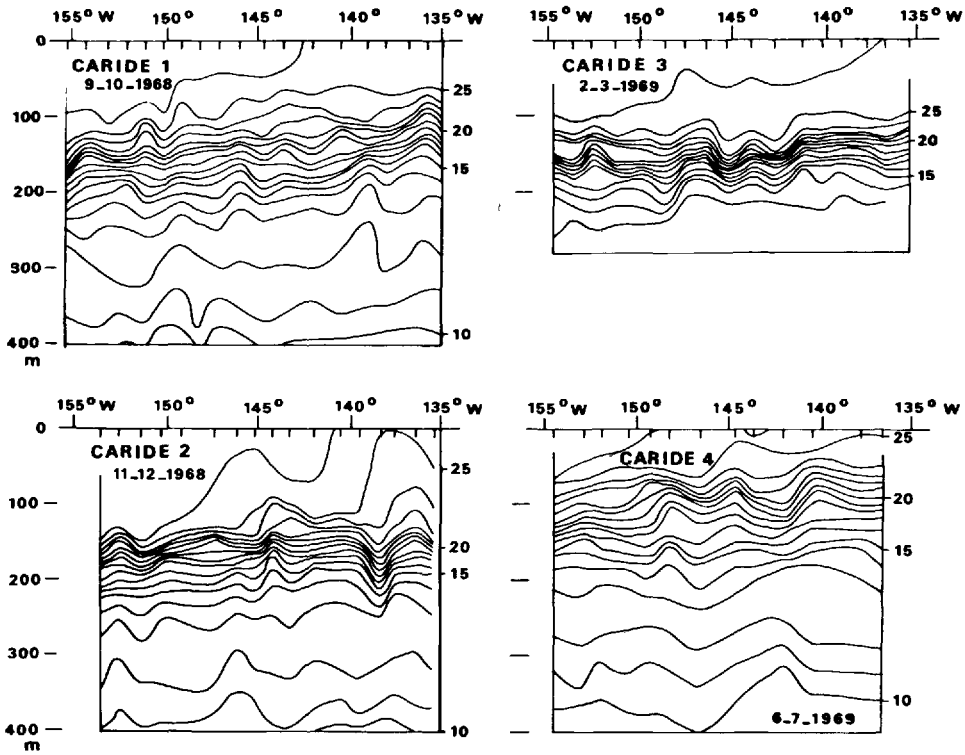

Figure 1. Distribution of the temperature with depth along the equator during the cruises *Caride* 1, *Caride* 2, *Caride* 3, *Caride* 4, *Caride* 6, and *Cassiopee* and *Aliopee*.

Dynamic height of the surface relative to 400 decibars was calculated for each equatorial section. The values were averaged for the band 2N–2S whenever data were available. The zonal pressure gradient γ was calculated following the method of Katz *et al.* (1977). A positive value of γ indicates increasing pressure toward the west. The wind stress was calculated by standard procedures which have been discussed by Wyrtki and Meyers (1976). Wind observations taken during the cruise were used, with the exception of the composite cruise of 1961, in which case Wyrtki and Meyers' wind data were used. The wind stress (T_x) was averaged over the same band of longitude as the hydrographic section. The synchronous values of T_x and γ for each cruise are given in Table 1.

A scatter diagram (Fig. 2) shows the statistical relationship between γ and T_x. The correlation coefficient (0.51) is significant, but also suggests that some variance is associated with internal waves or with low frequency transients. A very exceptional case is the 1958 *Igy* cruise when the pressure gradient reversed in the western Pacific, even though the easterly wind was still blowing. The 1976 *Eponite* cruise observed a small positive pressure gradient during a period of very weak westerly wind. The

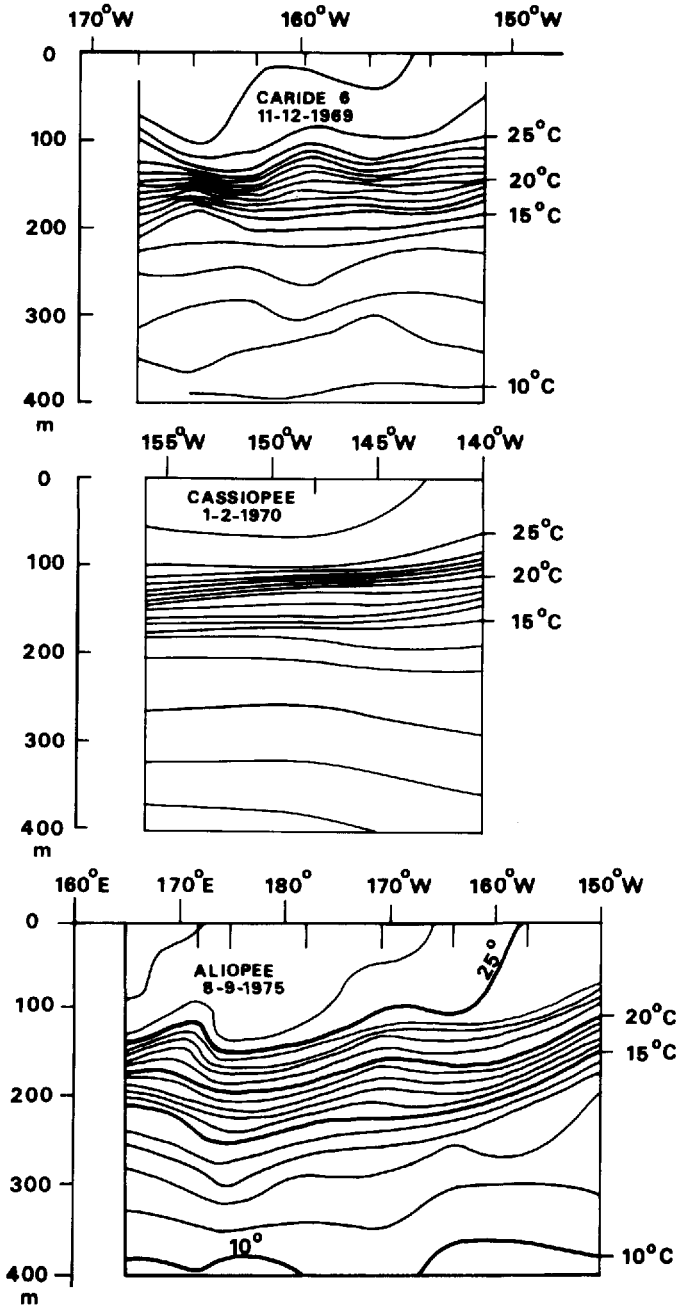

Figure 1. (Continued)

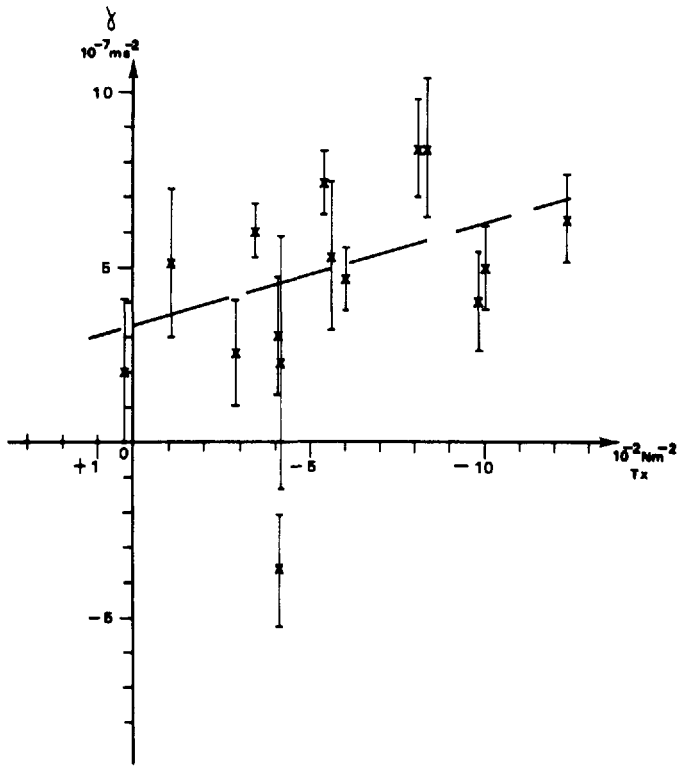

Figure 2. Correlation between the zonal pressure gradient γ and the zonal wind stress T_x during equatorial cruises. Vertical lines show 95% interval of confidence.

regression line does not pass through the origin apparently because the equatorial Pacific usually does not have time to completely relax to a state of equilibrium during periods of weak or null easterly wind stress. Several months or more would be required to establish an equilibrium (Philander, 1979). If $T_x = .05$ Nm^{-2} is representative of the long term mean wind stress (Meyers, 1979), then an equilibrium value of $\gamma = 4.8$ 10^{-7}ms^{-2} and the effective depth for the wind stress is 104 m. This is nearly the same effective depth estimated for the Atlantic by Katz *et al.* (1977).

The combination of all data suggests seasonal variations of zonal pressure gradient (Fig. 3). The large values during the latter half of the year were all observed in the central Pacific while the low values were observed in the western Pacific. Thus there is a trend for maximum gradient in September–October and minimum gradient after February in the central region; however, this seasonal signal has substantial interannual variations. The phase is the same as that described for the Atlantic by Katz *et al.* (1977).

The sequence of *Caride* and *Cassiopee* cruises provides six zonal sections on the

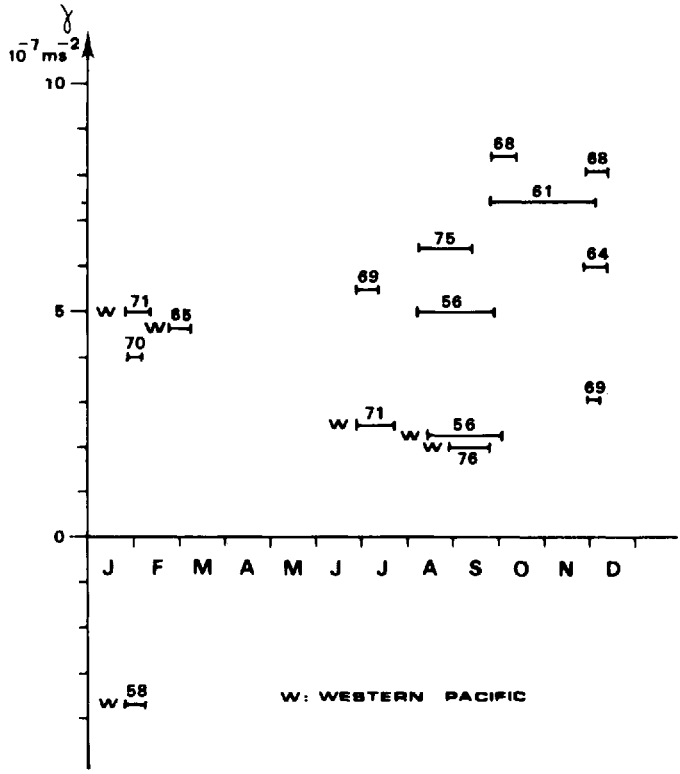

Figure 3. Distribution in time of the zonal pressure gradient. The horizontal lines span the observational periods of data. The year of each observation is noted.

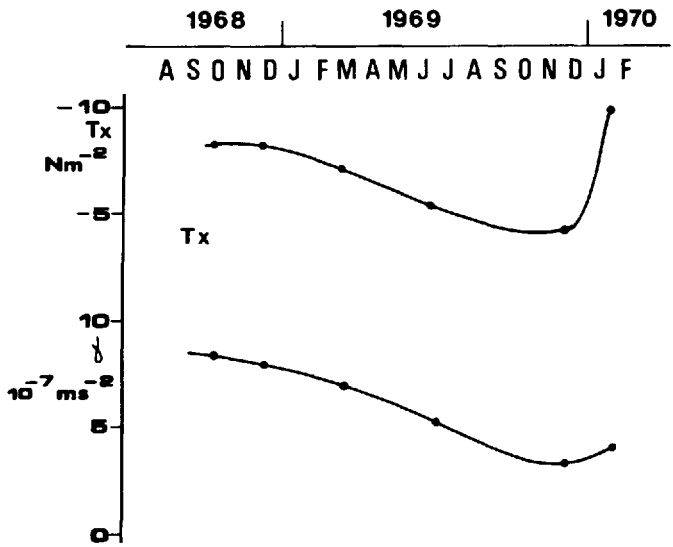

Figure 4. Evolution with time, from 1968 to 1970, of the zonal wind stress and of the zonal pressure gradient along the equator.

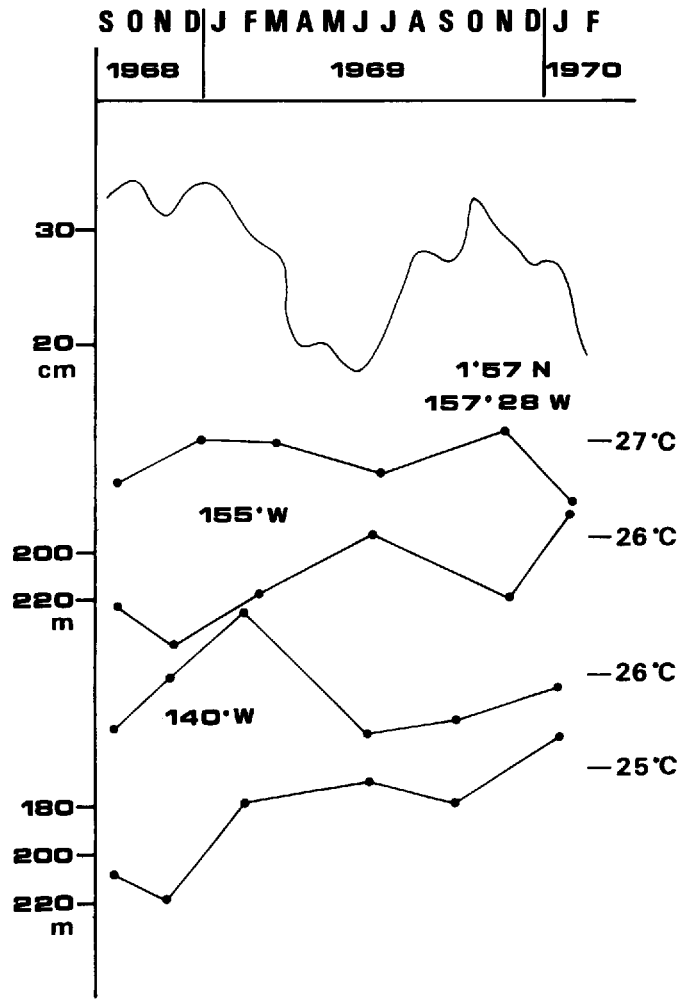

Figure 5. Evolution with time of the sea level at Christmas Island (1°57′N, 157°28′W) of the 14°C isotherm depth and sea-surface temperature at 155W and 140W.

equator which permit a more detailed description of variability during September 1968 to February 1970 (Fig. 4). The easterly wind stress and zonal pressure gradient follow the same trend of decreasing value from September 1968 until the end of 1969, followed by increasing values in February 1970. The depth of the thermocline and sea level at Christmas Island (Fig. 5) show the expected inverse relationship to each other, but they are not in phase with the wind stress and zonal pressure gradient. On the other hand, clearly the depth of the thermocline influences SST. The very large spatial scale (>2000 km) of these relationships is shown in Figure 1.

Variability of the four parameters can be synthesized (Table 2) as follows. In

Table 2.

	Dec 1968	June 1969	Dec 1969	Feb 1970
Mean sea level	High	Low	High	Low
Thermocline	Deep	Shallow	Deep	Shallow
Wind stress	Strong	Weak	Weak	Strong
Pressure gradient	Strong	Weak	Weak	Increasing

December 1968, strong wind stress and large pressure gradient are consistent with a local balance, while high sea level and deep thermocline suggest strong easterly wind stress farther east. In June 1969, the opposite situation is observed in all parameters, indicating a widespread relaxation of the wind and current system. By December 1969, the sea level and depth of the thermocline return to high values suggesting the importance of nonlocal effects, perhaps excited by remote winds, while the wind stress and pressure gradient remain locally balanced at low levels. In February 1970, the four parameters suggest a transient situation beginning to respond to re-establishment of the easterly wind system. The variations of wind stress and depth of the thermocline observed in 1968–1969 do not agree with typical seasonal variability as described by

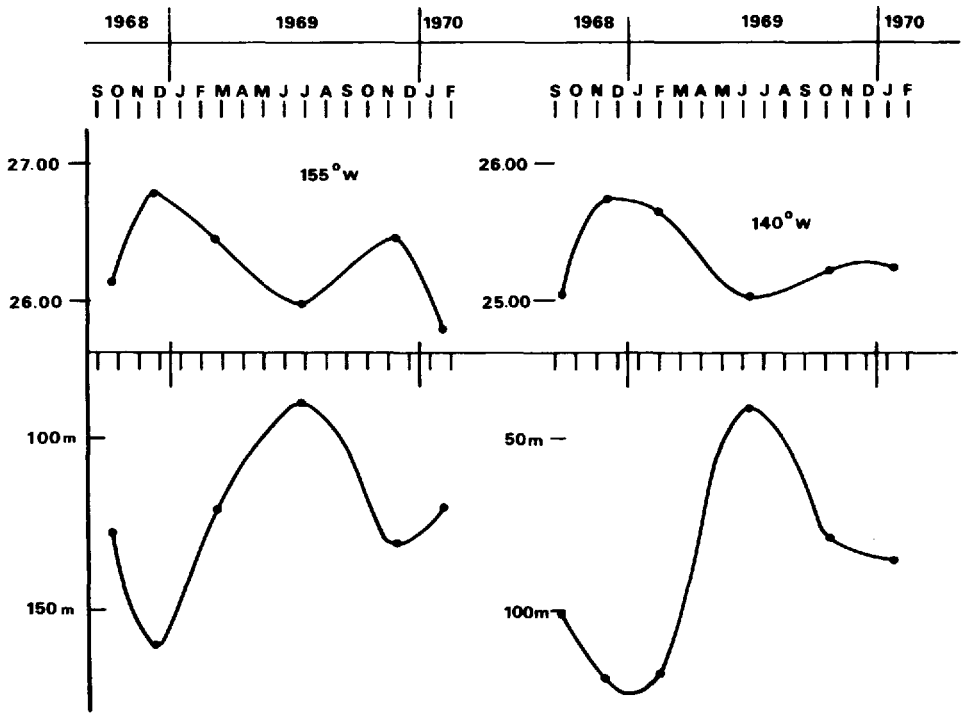

Figure 6. Variations 1968–1970 of the heat content at 155W and 140W as the mean temperature between sea surface and 24°C depth expressed in degree celsius (up) and variations 1968–1970 of the 24°C isotherm depth in meters (down).

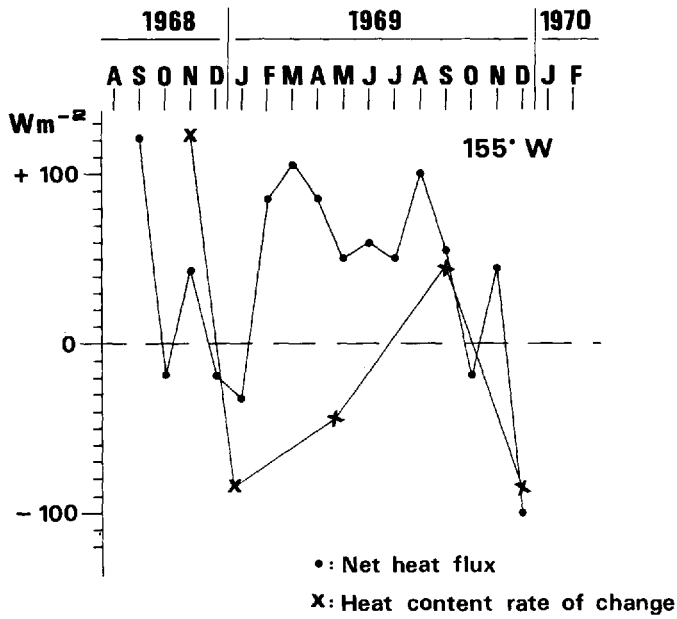

Figure 7. Net heat flux through the surface and observed rate of heat storage at 155W on the equator during the *Caride* and *Cassiopee* cruises. Heat storage was estimated following the method of Stevenson and Niiler (1983).

Meyers (1979). In 1969–1970, the pressure gradient in the central Pacific does not show either a strong seasonal variability (Fig. 3), and keeps a small value, as observed in the western Pacific. These features show that anomalous conditions persisted along the equator from 1968 to 1970.

3. Heat content and surface fluxes

The *Caride* and *Cassiopee* cruises are used in this section to study the relationship of mixed-layer heat content to surface fluxes. Heat content has been calculated as the vertically averaged temperature between the surface and the depth of 24°C, which reduces the contribution of adiabatic motions to the heat budget (Stevenson and Niiler, 1983). The heat content (Fig. 6, top) decreases during the early part of 1969 as observed by *Caride* 2, 3 and 4. Subsequently, it increases then decreases again, as observed during the last two cruises. These changes are exactly inverse to the depth of 24°C (Fig.6, bottom). These relationships also have a large spatial scale (Fig. 1). It is worth noting that Figures 5 and 6 together show that all of the isotherms from 14°C to 24°C have the same phase of depth.

The contribution to heat content variations by heat flux through the sea surface can be estimated. The net monthly heat flux in a 10°-longitude by 5°-latitude region centered at 0–155W from September 1968 to February 1970 is given in Figure 7 from

calculations made by Weare *et al.* (1981), together with an estimate of the rate of change of heat content between each cruise.[3] The order of magnitude of the heat flux fluctuations is ± 100 W m^{-2}, which is compatible with the observed rate of change in heat content. However, a comparison of the time series shown by Figure 7 points out that these two variables are not well correlated. While the heat content decreases (variation rate <0) during early 1969, the heat flux into the ocean is at a relative maximum. The difference in heat flux from late-1968 to mid-1969 barely exceeds the errors of such observations (Weare, personal communication); nevertheless the discrepancy seems to be real because of the much smaller month to month variation and because of the relatively frequent sampling at this location (the shipping lane between California and Australia). Only the decrease in heat content during early 1970 is related in a consistent way to the surface heat flux. This is in total contrast to conditions observed by Stevenson and Niiler (1983) in the same region during 1979/80 when fluxes and local heat storage were highly correlated during a 15 month period. Thus, many different processes can influence change in equatorial heat content on interannual time scales. The *Caride* cruises suggest that wind, possibly in a remote region, forces change in depth of the thermocline, which in turn alters heat content, and sea-surface temperature. This process acts in addition to and may be dominant over the changes directly forced by fluxes. We have not determined if the residual between heat content and fluxes contains information on advection by zonal currents or upwelling and entrainment. This will be the subject of a subsequent study.

In summary, we can state that along the equator (135W–155W) from September 1968 to February 1970, meterorological and oceanographic conditions were different from the historic average (Meyers, 1979). These anomalies may be related to the occurrence during early 1969 of a weak El Nino in the eastern Pacific. This perturbation, possibly transmitted by equatorial waves has changed heat content in the central Pacific independently of the local wind and surface fluxes.

4. Heat distribution in the equatorial Pacific

In most of the considered cases (Fig. 2), the wind stress is westward (negative) and the pressure increasing westward (positive). These conditions are characteristics of pre-or onset of El Nino periods. Reversal of the wind and pressure gradient in the western Pacific is characteristic of mature El Nino periods, as shown by the estimates of γ and T_x for January–February 1958 and August–September 1976 in Table 1.

The heat content in the upper layer is considered as particularly interesting due to its importance in the ocean-atmosphere exchanges. Practically, heat is stored in the equatorial Pacific between the sea surface and the top of the thermocline, usually marked by 24°C isotherm. Typical heat distribution during onset period of El Nino is

3. As long term trends for these two variables are approximately the same, it is not necessary to remove them from the data to compare fluctuations.

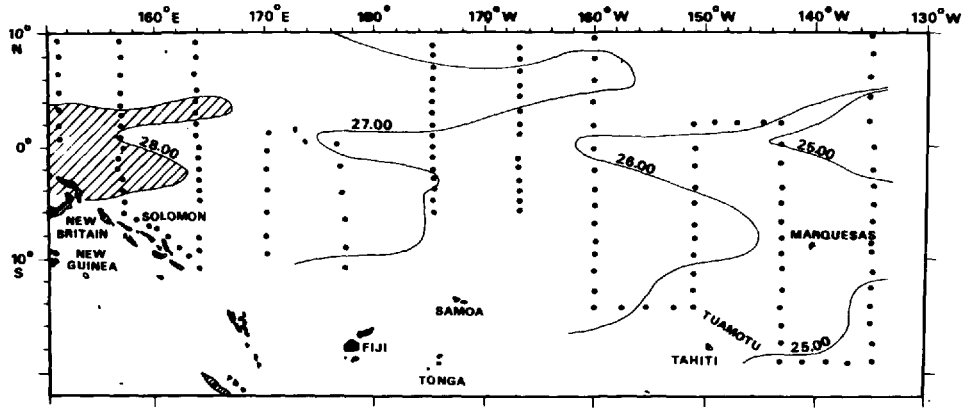

Figure 8. Distribution of the heat content as the mean temperature between sea surface and 24°C depth expressed in degree celsius during *Equapac* cruises in August–September 1956.

described by *Equapac* data (August–September 1956) (Fig. 8). A minimum of heat content due to equatorial upwelling occurs along the equator as far westward as 180° longitude. West of 170E, from 5N to 5S, the average temperature between the surface and the 24°C depth is more than 28°C. This maximum heat content has extensions each side of the equator; in the northern hemisphere at 5N this extension is probably

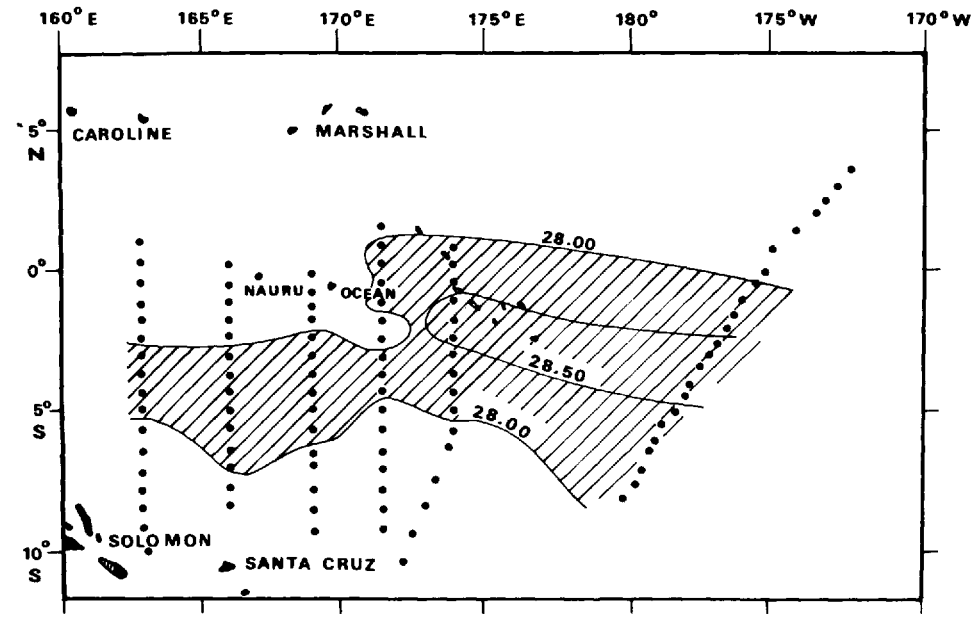

Figure 9. Distribution of the heat content as the mean temperature between sea surface and 24°C depth expressed in degree celsius during *Eponite* 2 cruises in September 1976.

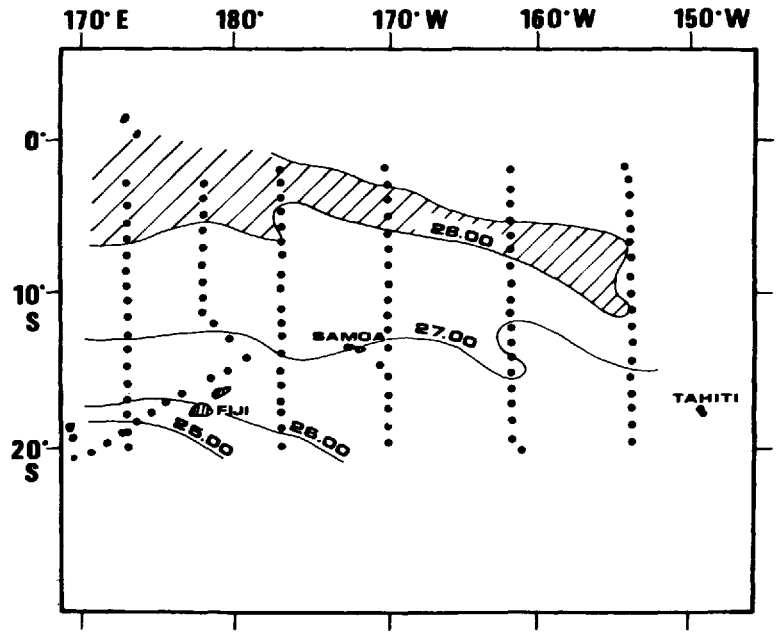

Figure 10. Distribution of the heat content as the mean temperature between sea surface and 24°C depth expressed in degree celsius, January–July 1977.

connected to the northern summer; surprisingly, extension also occurs in the southern hemisphere.

During mature El Nino periods, data are available for 1976 and 1957 events. For August to November 1976, a few months after the El Nino peak, data are available from *Eponite* 2 (Table 1) and a transequatorial XBT transect by the Coast Guard Vessel *Burton Island* (G. Seckel, personal communication). Weak west wind prevailed along the equator and the pressure gradient was weak. Thus, Figure 9 shows that another kind of heat distribution occurs in the equatorial Pacific. Maximum heat content lies in the central Pacific instead of in the western Pacific with average temperature from sea surface to 24°C depth of more than 28°C. Two other tropical cruises (*Danaides* 2 in January–February 1977 and *Ecoton* in June–July 1977) carried out by the Centre ORSTOM de Noumea from 20S to 3S, confirm this distribution of heat content during the mature El Nino situation (Fig. 10). The heat pool, located in the western Pacific before El Nino (Fig. 8), is now located in the central Pacific east of 180° longitude between 10S and the equator. A section along the equator during the mature phase of the 1957–8 event is available in the *Igy* data (Fig. 11). The pressure gradient was reversed in the western Pacific due to weak winds, and consequently the thermocline sloped downward to the east. This eastward slope of the thermocline is consistent with the shallowing of the thermocline observed after El Nino west of 180°

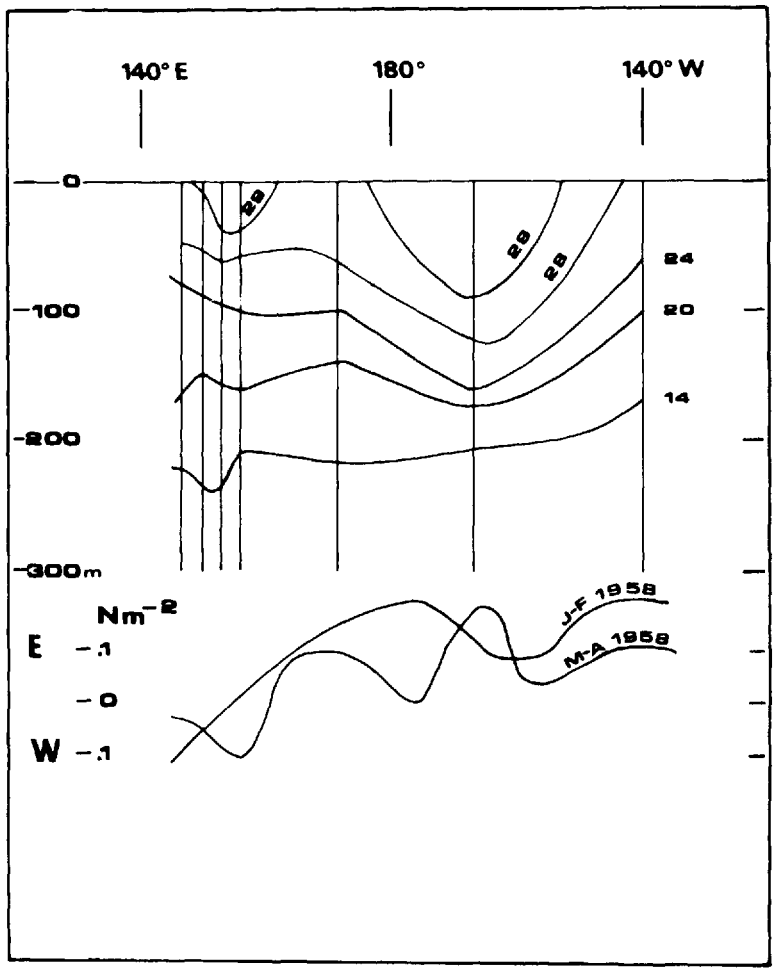

Figure 11. Equatorial profile of the isotherms along the equator during *Igy* 1958 cruises and wind stress in N m^{-2} in January–February and March–April 1958 (from Wyrtki and Meyers, 1976).

(Donguy *et al.*, 1982). The resulting heat content distribution (Fig. 12) presents a near equatorial minimum west of 180° and a maximum in the central Pacific between 10S and the equator and from 170E and 140W. East of 150W, another minimum occurs due to the remaining equatorial upwelling.

In fact, as already pointed out by Hénin and Donguy (1980) by consideration of the shallowest 100 meters depth, there are two kinds of heat distribution between the sea surface and the thermocline in the equatorial Pacific. In pre-El Nino period, the center of the heat pool is mainly located west of 180° (Fig. 8). In post-El Nino period, it is located in the central Pacific (Fig. 12).

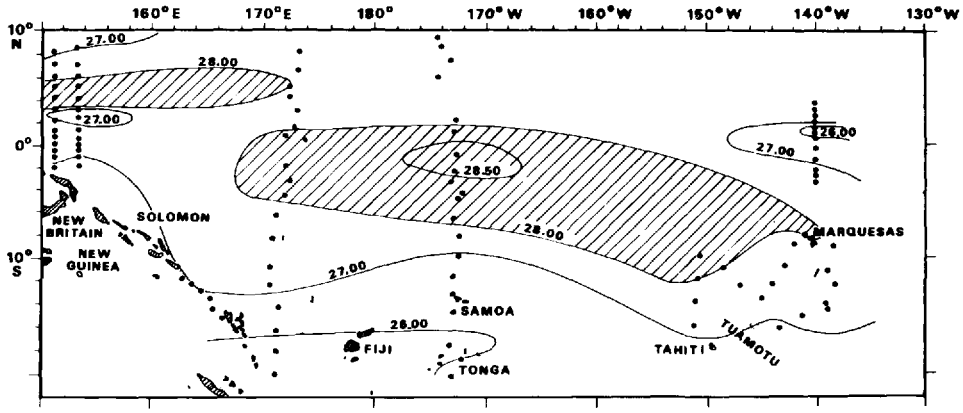

Figure 12. Distribution of the heat content as the mean temperature between sea surface and 24°C depth expressed in degree celsius, November 1957–March 1958 (*Igy* cruises).

5. Connection of the heat pool with convection in the West Pacific

Changes in large-scale convection patterns may be deduced from equatorial rainfall data. Seventeen (17) equatorial or almost equatorial stations have been considered (Table 3) covering the Pacific and Indian Ocean from South America to Africa. The spatial coverage is adequate, except from 90W to 155W where there are no stations. The monthly rainfall of each station is smoothed with a three month running mean and its ratio to the average is calculated. Figures show only positive rainfall anomalies. Three periods are considered: 1956–1959 (Fig. 13) with the occurrence of the 1957 El Nino; 1971–1974 (Fig. 14) with the occurrence of the 1972 El Nino; 1975–1978 with the occurrence of the 1976 El Nino (Fig. 15).

As already pointed out by Rasmusson and Carpenter (1981), in each case of El Nino, strong rainfall occurs at the same time during the second part of the year from

Table 3.

Guayaquil	02° 12 S	79° 50 W	Singapore	01° 22 N	103° 55 E
Cristobal	00° 54 S	89° 34 W	Colombo	06° 54 N	79° 52 E
Pampa Mia	00° 51 S	89° 28 W	Trivandrum	08° 29 N	76° 57 E
Christmas	01° 59 S	157° 29 W	Hulule	04° 11 N	73° 32 E
Fanning	03° 51 N	159° 22 W	Mahe	04° 37 S	55° 27 E
Canton	02° 46 S	171° 43 W	Aldabra	09° 25 S	46° 20 E
Tarawa	01° 21 N	172° 56 E	Monbasa	04° 05 S	38° 38 E
Ocean	00° 54 S	169° 33 E			
Nauru	00° 34 S	166° 55 E			
Momote	02° 03 S	147° 26 E			
Biak	01° 08 S	136° 06 E			
Mapia	00° 50 N	134° 18 E			

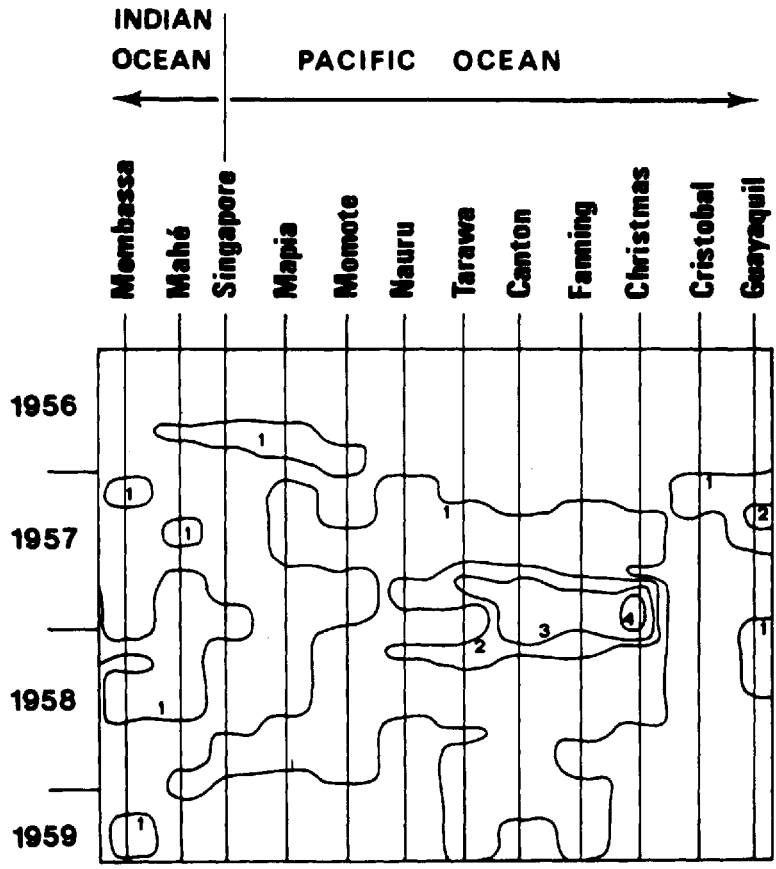

Figure 13. Ratio of the 1956–1959 rainfall to the average.

Tarawa to Christmas (from 180° to 160W), starting in September 1957, July 1972 and May 1976, with 3 times the average. By consideration of the outgoing longwave radiation anomalies, Heddinghaus and Krueger (1981) show similar features during 1976–77 with maximum negative anomalies suggesting rainfall close to the date line. The pattern of the 1957–58, 1972–73, and 1976–77 rainfall is consistent with the hypothesis of a splitting in two of the great Pacific Walker cell. The equatorial rainfall maximum would reveal the location of the ascending branch of the Walker cells and, conversely, minimum rainfall would indicate the position of the descending branch. The 1972 pattern (Fig. 14) could be interpreted as three Walker cells in the Pacific and Indian Oceans: one clockwise (as seen from the Southern Hemisphere) above eastern Pacific from South America to roughly 180° longitude; a second one, counterclockwise, above western Pacific and eastern Indian Ocean and the third one, clockwise again, above western Indian Ocean until Africa.

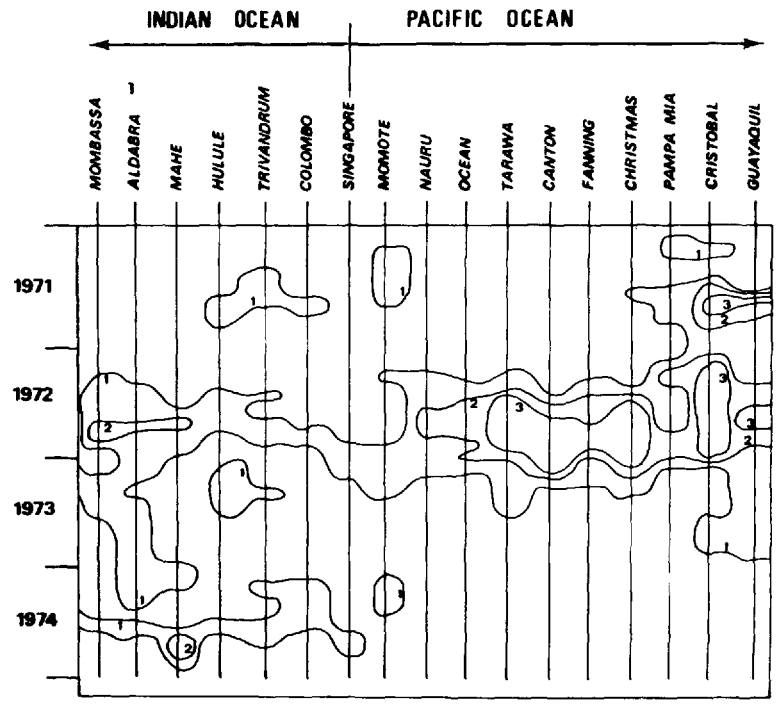

Figure 14. Ratio of the 1971–1974 rainfall to the average.

6. Conclusion

All of the ocean/atmosphere variables discussed in this article can be synthesized into a scenario of large-scale air/sea interaction. Before El Nino periods, strong easterly wind blows along the entire equator of the Pacific Ocean from America to Indonesia. The pressure gradient in oceanic surface waters is positive, and consequently the thermocline slope is westward, with its depth increasing from 50 m or less in the east to 200 m in the west. During El Nino periods, westerly wind blows in the western Pacific while easterly wind still prevails in the eastern Pacific. The pressure gradient reverses west of the dateline but not farther east. Consequently, the thermocline bows downward in the central Pacific, in the region between easterly and westerly winds. The Pacific heat pool is then located east of the dateline where the thermocline is the deepest.

The importance of the heat pool is that it fixes a location where conditions are favorable for convergence of the surface winds. A region of deep cumulus convection is always located above the heat pool, where surface temperatures and evaporation are maximum. For this reason the convection is located in the western Pacific before El Nino, and it has seasonal variations following the sun into the summer hemisphere. After El Nino, convection is still located above the heat pool, but it is shifted into the

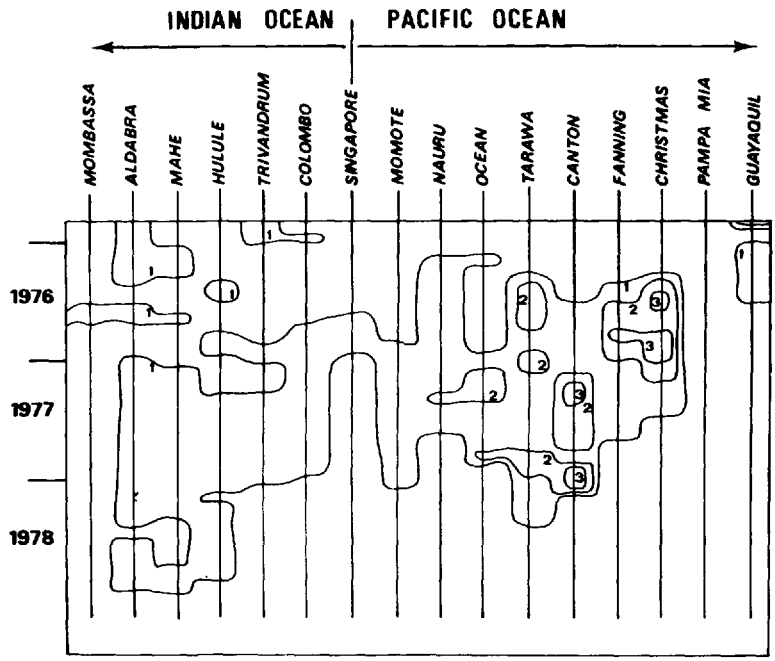

Figure 15. Ratio of the 1975–1978 rainfall to the average.

central Pacific close to the equator between 0° and 10S (Figs. 10 and 12), where the ascending branch of the Walker cell is located and anomalous rainfall is observed (Bjerkness, 1969; Krueger and Gray, 1969). Along the Pacific equator, there are then two Walker cells: the eastern one is still clockwise but the western one is anticlockwise. Little is known about the mechanism which connects convection to the heat pool. The convection zone is the preferential location for rainfall and release of latent heat; however, the relative importance of local evaporation and large-scale vapor flux convergence is difficult to estimate with existing data (Rasmusson and Carpenter, 1982).

A schematic picture may be drawn (Fig. 16) to summarize the essential features of atmosphere/ocean coupling before and after El Nino episodes. During pre-El Nino periods, the equatorial surface wind is westward inducing westward isotherm slope and also westward current above the thermocline. Heat content is concentrated in the western Pacific inducing atmospheric convection and formation of the ascending branch of the Walker cell. During post-El Nino, surface wind and surface current are reversed in the western Pacific, but not in the eastern Pacific. As eastward wind induces shoaling of the thermocline in the west (Donguy *et al.*, 1982), the process of heat storage in the central Pacific is enhanced. Several processes act together to form maximum surface temperature near the dateline: weak winds reduce upwelling

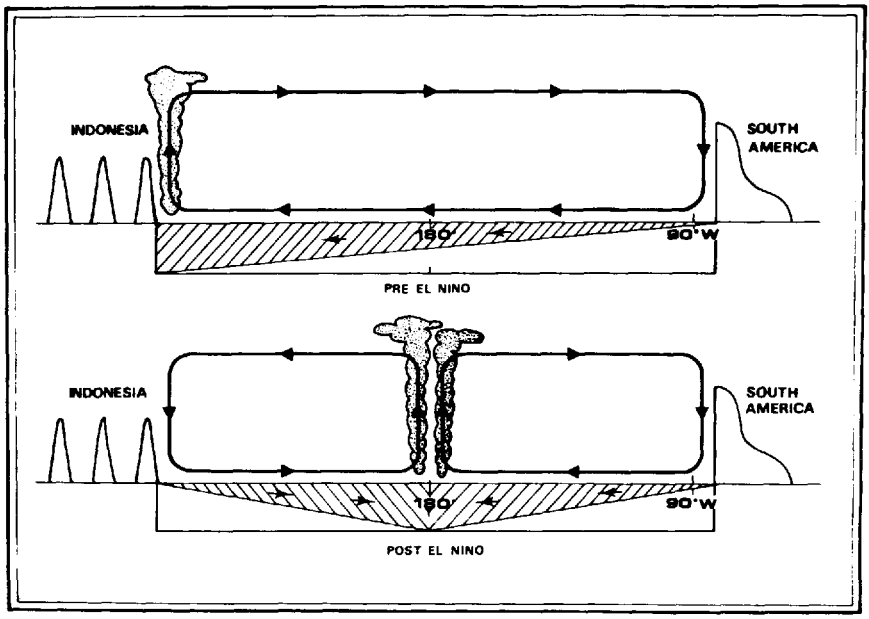

Figure 16. Hypothesis of the splitting of the Walker cell. Shaded area is the maximum of heat content.

velocities, while depression of the thermocline limits availability of cold water; weak winds reduce evaporation while insolation warms the motionless surface water, located between easterly and westerly winds. Consequently heat is concentrated in a thick layer in the central Pacific, and induces convection and formation of the ascending branch of the eastern and western Walker cells. The hypothesis of the splitting of the Walker cell is probably too simple to be realistic; however it is consistent with most of the features observed in the equatorial area before and after El Nino. Thus the illustration suggests a hypothesis for the mechanism by which the equatorial ocean and atmosphere become "locked" into an anomalous pattern during El Nino periods. The mechanism which forces the zone of deep cumulus convection to form above the heat pool needs further study to understand if positive feedback from ocean to atmosphere is occurring locally.

Acknowledgments. Part of this research was supported by the National Science Foundation under grants to the NORPAX and PEQUOD programs. This support is gratefully acknowledged.

REFERENCES

Anonymous. 1980, 1981. Resultats des croisières faites par le Centre ORSTOM de Noumea—Rapport Scientifique et Technique, No. 12, 13, 15, 16.

Bjerkness, J. 1969. Atmospheric teleconnections from the equatorial Pacific. Mon. Wea. Rev., 97, 163–172.

Donguy, J. R., C. Henin, A. Morliere and J. P. Rebert. 1982. Thermal changes in the western tropical Pacific in relation to the wind field. Deep-Sea Res., *29,* 869–882.

Emery, W. J. 1976. The role of vertical motion in the heat budget of the upper northeastern Pacific Ocean. J. Phys. Oceanogr., *6,* 299–305.

Halpern, D. 1980. A Pacific equatorial temperature section from 172E to 110W during winter and spring 1979. Deep-Sea Res., *27,* 931–940.

Heddinghaus, T. R. and A. F. Krueger. 1981. Annual and interannual variations in outgoing longwave radiation over the tropics. Mon. Wea. Rev., *109,* 1208–1218.

Hénin, C. and J. R. Donguy. 1980. Heat content changes within the mixed layer of the equatorial Pacific Ocean. J. Mar. Res., *38,* 767–780.

Katz, E. J. and Collaborators. 1977. Zonal pressure gradient along the equatorial Atlantic. J. Mar. Res., *35,* 293–307.

Krueger, A. F. and T. G. Gray. 1969. Long-term variations in equatorial circulation and rainfall. Mon. Wea. Rev., *97,* 700–711.

Lemasson, L. and B. Piton. 1968. Anomalie dynamique de la surface de la mer le long de l'equateur dans l'Ocean Pacifique. Cah. ORSTOM, sér. Océanogr, *6,* 39–45.

Masuzawa, J. and K. Nagasaka. 1975. The 137E oceanographic section. J. Mar. Res., *33,* (Suppl.), 109–116.

Merle, J. 1980a. Seasonal heat budget in the equatorial Atlantic Ocean. J. Phys. Oceanogr., *10,* 464–469.

——. 1980b. Seasonal variation of heat-storage in the tropical Atlantic Ocean. Oceanol. Acta, *3,* 455–474.

Meyers, G. 1979. Seasonal variation in the slope of the 14°C isotherm along the equator in the Pacific Ocean. J. Phys. Oceanogr., *9,* 885–891.

Philander, S. G. H. 1979. Variability of the tropical oceans. Dyn. Atmos. Ocean., *3,* 191–208.

Quinn, W. H., D. O. Zopf, K. S. Short and R. T. W. Kuo Yang. 1978. Historical trend and statistics of the Southern Oscillation, El Niño, and Indonesian droughts. Fish. Bull., *76,* 663–678.

Rasmusson, E. and T. Carpenter. 1982. Variations in tropical sea surface temperature and surface wind fields associated with the Southern Oscillation/El Niño. Mon. Wea. Rev., *110,* 354–384.

Stevenson, J. W. and P. P. Niiler. 1983. Upper ocean heat budget during the Hawaii to Tahiti Shuttle Experiment. J. Phys. Oceanogr., (in press).

Weare, B. C. 1983. Interannual variation in net heating at the surface of the tropical Pacific Ocean. J. Phys. Oceanogr., *13,* 873–885.

Weare, B. C., P. T. Strub and M. D. Samuel. 1981. Annual mean surface heat fluxes in the tropical Pacific Ocean. J Phys. Oceanogr., *11,* 705–717.

White, W. B. and K. Hasunuma. 1980. Interannual variability in the baroclinic gyre. J. Phys. Oceanogr., *6,* 299–305.

Wyrtki, K. and G. Meyers. 1976. The trade wind field over the Pacific Ocean. J. Appl. Met., *15,* 698–704.

Received: *1 June, 1983;* revised: *10 November, 1983.*